Electrical and Quench Performance of the First MICE Coupling Coil

Michael A. Tartaglia, Ruben Carcagno, Andrzej Makulski, J. Nogiec, Darryl Orris, Roman Pilipenko, Cosmore Sylvester, Shlomo Caspi, Heng Pan, Soren Prestemon, Steve Virostek

***Abstract*— The first MICE Coupling Coil has been tested in a conduction-cooled environment in the new Solenoid Test Facility at Fermilab. We present an overview of the power and quench protection scheme, and report on the electrical and quench performance results obtained during cold power tests of the magnet.**

***Index Terms*—Superconducting Solenoid, Quench Protection, Quench Performance.**

I. Introduction

The MUON Ionization Cooling Experiment, MICE, is a multi-stage engineering effort to demonstrate ionization cooling of a muon beam at Rutherford Appleton Laboratory (RAL) in the UK [1]. The experiment depends upon a set of large superconducting magnets, two Spectrometer Solenoid (SS) magnets [2] for initial and final muon momentum analysis, and two high field Coupling Coil (CC) magnets [3] to control muon trajectories through RF cavities that will reaccelerate the muons, to restore longitudinal momentum lost by ionization of the medium. Quench re-training of both SS magnets has been completed recently, following some HTS lead repairs and cooling system improvements. The recent SS magnet tests were performed at the Wang, NMR fabrication site using a quench detection and data logging system developed at Fermilab [4], which will also be used for operating the SS magnets at RAL. This quench protection system was replicated for testing of large conduction cooled superconducting magnets in a new Solenoid Test Facility (STF) [5,6,7] which is located in the Central Helium Liquifier building (CHL) at Fermilab.

Design parameters of the Coupling Coil are shown in Table I. The first CC was wound by Qi Huan in China. LBNL performed final welding of the outer aluminum structure, pressure and leak tests of helium cooling channels, mounting and electrical connections of the protection diodes to 8 coil segments, and final electrical checks. Hipot tests of ground insulation revealed leakage current, and thereafter tests were restricted to 250 V warm, and 150 V cold. The coil was shipped to Fermilab in January 2013 for testing in the STF, where it also passed these same tests numerous times during the coil qualification program.

TABLE I
PARAMETERS OF THE MICE COUPLING COIL

Parameter	Specification
Coil Design	96 layers, 166 turns per layer
Superconductor Strand	Cu/NbTi (MRI) 1.0 mm x 1.65 mm
Structure Outer Diameter	1860 mm
Magnet Weight	2.2 Tons
Cryogenic Cooling	Conduction Cooled
Magnet Inductance	596 H
Maximum Current (4.5K)	220 A
Stored Energy (220 A)	14.4 MJ
Peak Field on coil 1 (220 A)	7.5 T
Peak Field on axis (220 A)	2.6 T

II. Test Program Overview

The MICE experiment has several configurations, which require the CC reach a minimum current of 175 A and maximum of 210 A. The main test program goal was to train the CC to 214 A, then demonstrate stable operation for 24 hours (known as a "soak" test), to qualify the bare coil for use in MICE prior to installation into a dedicated cryostat. It was also important to evaluate the retraining after a thermal cycle, characterize the performance of the diode protection scheme, and benchmark quench development simulations [8].

As discussed in [6], to achieve the required operating temperatures in this new facility took a number of iterations and improvements. An estimated coil temperature of 5.5 K is required to reach 214 A. The coil reached 9 K during first cool down, or thermal cycle (TC). After the first set of stand and insulation modifications, coil surface temperatures ranged from 6 to 8 K and three training ramps resulted in identical quenches at 62 A, consistent with a thermal limitation in TC2.

Significant improvements made training to high current possible in TC3, reaching 194.5 A with a peak temperature of 5.7 K, and limited by uncontrolled temperature excursions of the 2-phase helium system. Fig. 1 shows the temperature and current ramp profiles for this event; one can see the heating effects of eddy currents in the aluminum structure. The warmest temperatures were at the lead connections (no lead quenches occurred). Fig. 2 shows the correlation of quench current with the peak surface temperature, a proxy for the peak coil temperature (not measured directly), and clear boundary for the coil critical surface that would limit further training.

Automatically generated dates of receipt and acceptance will be placed here; authors do not produce these dates. This work was supported by Fermi Research Alliance, LLC, under contract No. DE-AC02-07CH11359 with the U.S. Department of Energy.

M. Tartaglia, R. Carcagno, A. Makulski, J. Nogiec, D. Orris, R. Pilipenko, and C. Sylvester are with Fermi National Accelerator Laboratory, Batavia, IL 60510 USA, e-mail: tartaglia@fnal.gov.

S. Caspi, H. Pan, and S. Virostek are with Lawrence Berkeley National Laboratory, Berkeley, CA

After warming to room temperature the quench re-training study was then started in TC4, but was interrupted by a broken compressor piston. While this was repaired the coil again reached 300 K, and second re-training study was made in TC5. The final ramp included a 2 hour "soak test" at 175 A with a ramp to 193 A.

The quench training history for TC3-5 is shown in Fig. 3. Clearly the training was slow but steady, and re-training was fast – above the minimum 175 A operating point. Most quenches occurred in the high field regions (coils 1,8), and two quenches occurred elsewhere.

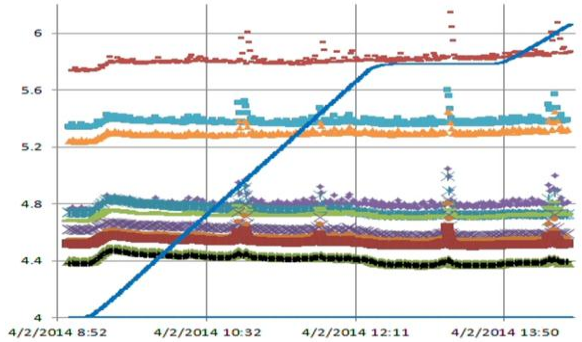

Fig. 1. Coil surface temperatures and current during ramp to 194.5 A quench. Current was held at 170 A for one hour. Eddy currents in the aluminum structure cause the temperatures to all rise slightly; they slowly decline as the eddy current loops are limited by increasing field strength.

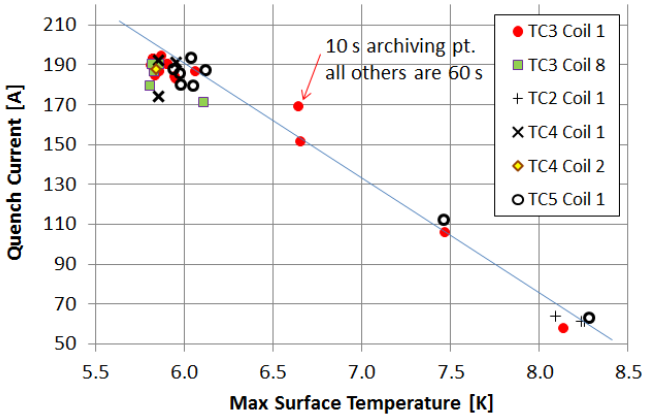

Fig. 2. Quench current versus peak surface temperature (measured by two synchronized systems).

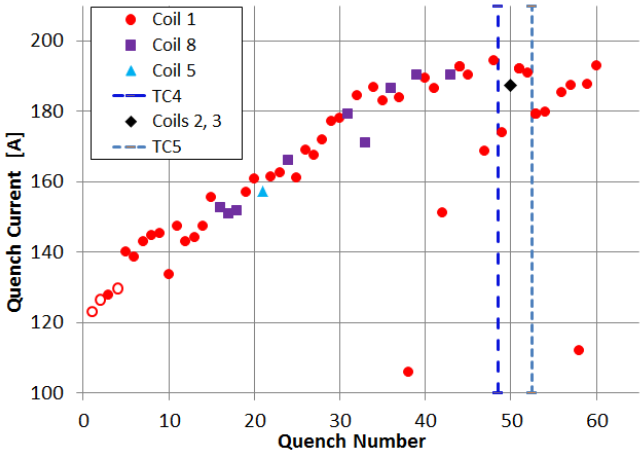

Fig. 3. Quench History of the MICE CC, beginning with the thermal cycle 3.

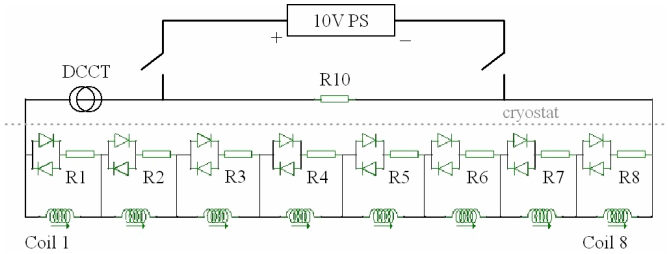

Fig. 4. Power and quench protection circuit for the MICE CC in the initial polarity configuration at STF. Resistances R1 to R8 are zero, while the external resistor R10 is 2 Ω for the test.

III. Quench Protection and Power System

Fig. 4 shows the electrical circuit for the test at STF. There are eight sub-coils of 12 layers, each protected by a pair of opposed diodes; resistances in the coil circuit were parameters in earlier quench protection simulations. A CC quench simulation model, which had previously been compared to other models [9], was created at LBNL utilizing Vector Fields Opera 3D to simulate quench development; results for our test configuration are compared here to the test data.

Voltage taps connected across each of the coil segments are monitored by the quench protection and logging system [4], which captures the full magnet current and voltage history in a slow monitor data stream, and saving of fast sampled data in a window around the quench event. Quench detection (QD) by the FPGA-based system relies primarily on the difference of two "half-coil" voltage signals exceeding threshold for a specified validation time. In early training ramps the QD system was triggered by rapid voltage excursions (see Fig. 5) that recovered (presumably from coil motion) and did not necessarily develop into a quench – these are shown as open symbols in Fig. 3. The QD trigger was desensitized to nuisance trips by raising threshold to 4.5 V and requiring a 15 ms validation time after threshold crossing before reacting.

In addition to triggering fast data saving, the QD system disconnects the power supply from the coil by opening two mechanical relays. This causes the current to discharge through the R10 dump resistor, and the developed voltage is sufficient to force the (reverse polarity) diodes across all coils to conduct. Fig. 6 shows a typical quench development and detection event. Note that this differs from the nominal CC protection scheme in which forward resistive voltage in the

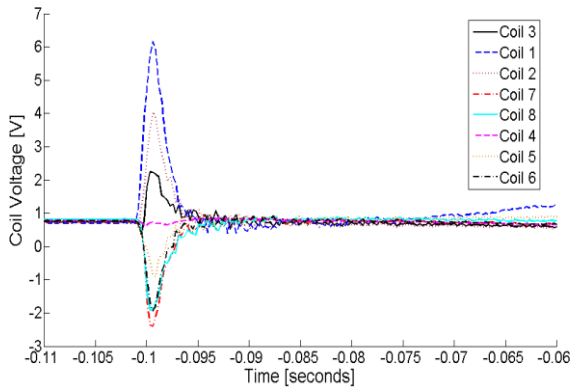

Fig. 5. Typical Fast Voltage Spike, one that did result in a coil 1 quench.

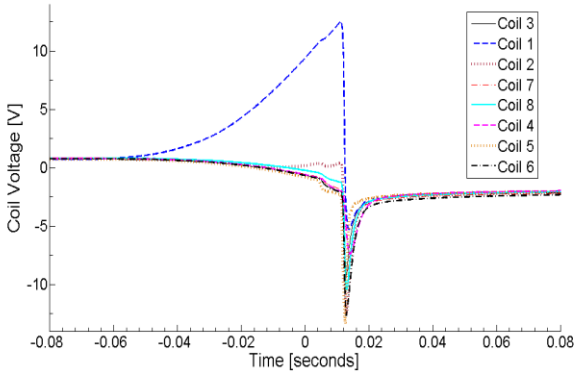

Fig. 6. Coil voltages during quench development of coil1, then coil 2, and following detection for highest current quench at 194.5A.

quenching coils causes the individual diodes to conduct.

The maximum output voltage of the power supply was 10 V; however, due to resistive losses of the bus and the dump resistor R10, the ramp rate of the 596 H load was limited to 15 mA/sec. Ramping to the expected operating current of 210 A would take ~4 hours, which made it impractical to quench the magnet more than once per day. Since the magnet was training very slowly it was desired to increase the ramp rate so the magnet could be quenched twice a day. This was achieved by replacing the Cryogenic power supply with two Lambda GEN10-330 power supplies connected in series, which doubled the available voltage to 20 V. Nevertheless, because the coil absorbs most of the stored energy, at high current thermal recovery from the quenches limited the test to one ramp per day.

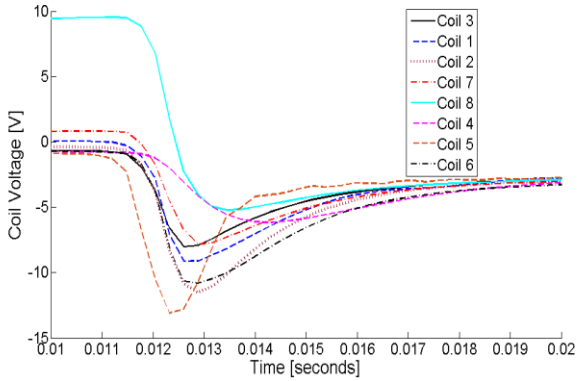

Fig. 7. Coil voltages just after a coil 8 quench detection, showing diode conduction due to reversed voltage across dump resistor. Delay after detection at t=0 is due to mechanical relays disconnecting the power supply.

IV. Diode Characteristics

In each thermal cycle, quench training was started only after verifying that the quench detection and diodes operated correctly. This was done by ramping to a low current and triggering the system manually (25 A), or by a film-heater induced quench (46 A). No problems were ever encountered with the system during these checkout tests, or subsequent training events.

Fig. 7 shows a typical example of the diode voltages after a quench, each starting to conduct at a particular voltage as the current flows in the reverse direction across the dump resistor; the voltages drop rather quickly to about -1 V as they heat up. Prior cold tests of MICE CC diodes at Fermilab [10] showed conduction starting at ~4.5 V, and increasing with magnetic field (esp. B⊥). Fig. 8 summarizes the behavior during the CC test for a sample of quench events in TC2-4. The data show variations of a few volts, and perhaps a trend of the turn-on voltage becoming slightly lower at higher field (or more cycles). In TC5, the power supply polarity was reversed to test the opposing set of diodes. Table II shows the measured voltage ranges (absolute values) observed for all diodes, by polarity. In TC5, the coil 5 diode conducted at nearly 30 V for several events, then consistently turned on at about 15 V.

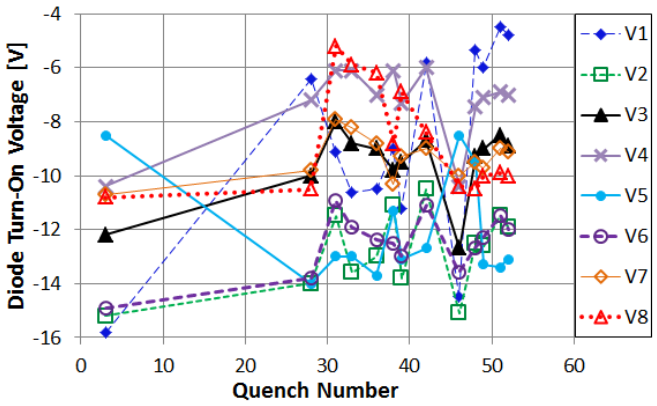

Fig. 8. Variation of diode turn-on voltages versus quench number in TC2-4 (initial polarity of current).

TABLE II
Diode Turn-On Voltage Ranges

Coil #	Initial Polarity (TC2,3,4)	Reversed Polarity (TC5)
1	4.5 - 15.8	6.2 - 13.5
2	10.5 - 15.2	5.3 - 9.4
3	8.0 - 12.7	9.2 - 10.7
4	6.0 - 10.4	5.1 - 8.4
5	8.5 – 14.0	13.8 - 29.5
6	10.9 - 14.9	8.0 - 9.6
7	7.9 – 10.7	11.2 – 16.1
8	5.2 - 10.8	6.6 – 11.0

Fig. 9 shows the distribution of the coil resistive voltages as a function of the quench current at the time of QD trigger. The values are typically above the levels (6-8 V) where they would be expected to conduct, but there was no evidence in any quench event of a diode conducting due to the forward resistive voltage prior to the QD trigger.

V. Quench Development

Once the diodes start to conduct, the current in each coil segment circulates locally and dissipates energy through eddy current coupling in the aluminum mandrel. A small fraction of the original current continues to flow through the dump resistor as well, until the diodes fall below their 1 V forward threshold. To monitor the quench development process, and allow comparison with simulations, a hall probe captured the fast field decay in the quench data. Normalized to the DCCT measured current, this is a good proxy for the average magnet current.

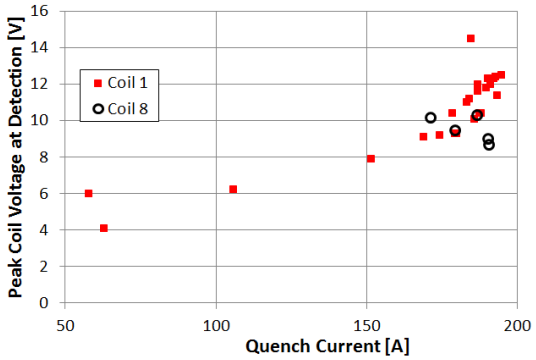

Fig. 9. Resistive voltage of quenching coil at the time of quench detection, as a function of the quench current.

As mentioned above, a simulation of the quench development using Vector Fields Opera 3D was performed, to calculate the time dependent coil currents and temperatures. A quench in the coil 1 high field region was simulated at several currents. The model assumed the circuit parameters of Fig. 4 and studied diode turn-on voltages ranging from 1.4 to 6 V. The calculated coil hot spot and peak surface temperatures are slightly dependent on this parameter (the latter corresponding to an average bobbin temperature in the region near the coil hot spot). In Fig. 10 the model results (6 V diode case) are compared to the measured peak surface temperatures observed after each quench. The agreement is quite good, and leads to confidence in the hot spot temperature calculation.

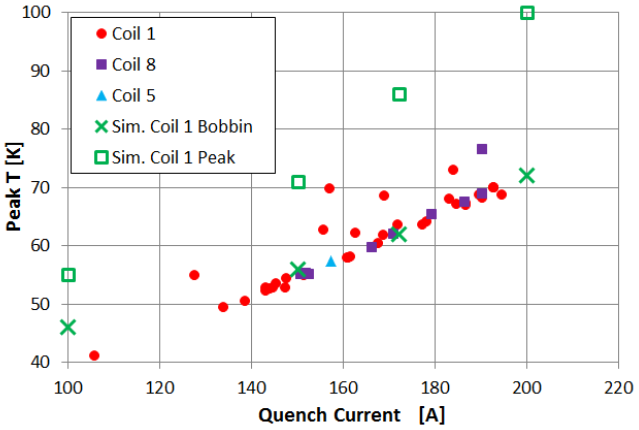

Fig. 10. Measured peak temperature on the bobbin surface after quench, and simulation of coil and bobbin temperatures, as a function of quench current.

Fig. 11 shows the comparison of the model prediction for individual coil currents with the scaled magnetic field following the quench at high current. Again we observe very good agreement, which further validates the model.

VI. Conclusion

The first MICE Coupling Coil test has been completed in the new Solenoid Test Facility at Fermilab. The magnet was trained to 195 A, a current well above the minimum 175 A required for MICE, although thermal conditions prevented reaching the 210 A maximum MICE current. The magnet re-training began above the 175 A value after each of two room temperature thermal cycles. The training was slow, and coil voltage signals (both quench and slow monitor) show

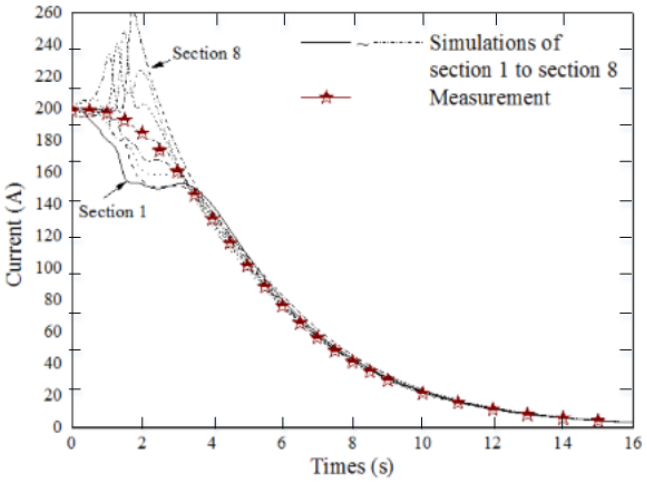

Fig. 11. Opera3D quench simulation of coil section currents for a 200A coil 1 quench, compared to measured (scaled) magnetic field decay profile for the 194.5 A highest current quench.

evidence of conductor motion, manifested as voltage spikes that occurred throughout the training. The coil experienced 60 quenches with no evidence of degradation.

The cold diode turn-on voltage characteristics differed from expectations based on performance tests previously conducted. The magnetic field dependence was a slight trend toward lower voltages with higher field, or perhaps the trend was due to conditioning with more cycles. Typically, voltages for individual diodes varied by only a few volts for most quenches. Forward diode conduction due to quench resistive voltage growth was not seen, although the data suggest that it likely should have occurred.

The quench and temperature data provided a good benchmark for the LBNL Opera3D quench simulation model, which gives good agreement with the measured peak aluminum structure surface temperature and with the decay of the average magnet current inferred from the magnetic field.

Acknowledgment

The authors wish to acknowledge the many contributions and strong support provided by the Fermilab Accelerator Division Cryogenics Department to the successful completion and operation of the new Solenoid Test Facility at CHL and MICE CC test program.

References

[1] http://www.mice.iit.edu/miceatral/
[2] V.Kashikhin, *et al.*, "Quench Analysis of MICE Spectrometer Superconducting Solenoid," *IEEE Trans. Appl. Supercond.*, vol. 22, no. 3, June 2012, 4702904.
[3] L. Wang, *et al.*, "The Engineering Design of the 1.5 m Diameter Solenoid for the MICE RFCC Modules," *IEEE Trans. Appl. Supercond.*, vol. 18, no. 2, June 2008, p937.
[4] R. Pilipenko, *et al.*, "An FPGA-Based Quench Detection and Continuous Logging System for Testing Superconducting Magnets," *IEEE Trans. Appl. Supercond.*, vol. 23, no. 3, June 2013, 9500503.
[5] R. Rabehl, *et al.*, "A Cryogenic Test Stand for Large Superconducting Solenoid Magnets," *Adv. In Cryogenic Engineering*, vol. 59A, pp 215-222, 2014.
[6] R. Rabehl, *et al.*, "Thermal and Mechanical Performance of the First MICE Coupling Coil and the Fermilab Solenoid Test Facility," submitted to ASC 2014.

[7] D. Orris, *et al.*, "A New Facility for Testing Superconducting Solenoid Magnets with Large Fringe Fields at Fermilab," Proceedings of NA-PAC13, THPBA16, Available: http://www.napac13.lbnl.gov/
[8] B. A. Smith, *et al.*, "Design and Analysis of the Quench Protection System for the MICE Coupling Coils," *IEEE Trans. Appl. Supercond*., vol. 23, no. 3, June 2013, 4700304.
[9] H. Pan, *et al.*, "A Comparison of the Quench Analysis on and Impregnated Solenoid Magnet Wound on an Aluminum Mandrel Using Three Computer Codes," *IEEE Trans. Appl. Supercond*., vol. 23, no. 3, June 2013, 4901005.
[10] V. Kashikhin, *et al.*, "MuCool Superconducting Solenoid Quench Simulations and Test Stand at FNAL," *IEEE Trans. Appl. Supercond*., vol. 23, no. 3, June 2013, 4101704.